Influence of Estrogens on GH-Cell Network Dynamics in Females: A Live *in Situ* Imaging Approach

Marie Schaeffer, David J. Hodson, Anne-Cécile Meunier, Chrystel Lafont, Jérôme Birkenstock, Danielle Carmignac, Joanne F. Murray, Elodie Gavois, Iain C. Robinson, Paul Le Tissier, and Patrice Mollard

Centre National de la Recherche Scientifique (M.S., D.J.H., A.-C.M., C.L., J.B., E.G., P.M.), Unité Mixte de Recherche (UMR)-5203, Institute of Functional Genomics; Institut National de la Santé et de la Recherche Médicale (M.S., D.J.H., A.-C.M., J.B., E.G., P.M.), Unité 661; and Universities of Montpellier 1 and 2 (M.S., D.J.H.,. A.-C.M., E.G., P.M.), UMR-5203, F-34000 Montpellier, France; Royal College of Surgeons in Ireland (M.S.), Dublin 2, Ireland; National Institute for Medical Research (D.C., I.C.R., P.L.T.), Division of Molecular Neuroendocrinology, London NW7 1AA, United Kingdom; and School of Life Sciences (J.F.M.), University of Westminster, London, W1W 6UW, United Kingdom

The secretion of endocrine hormones from pituitary cells finely regulates a multitude of homeostatic processes. To dynamically adapt to changing physiological status and environmental stimuli, the pituitary gland must undergo marked structural and functional plasticity. Endocrine cell plasticity is thought to primarily rely on variations in cell proliferation and size. However, cell motility, a process commonly observed in a variety of tissues during development, may represent an additional mechanism to promote plasticity within the adult pituitary gland. To investigate this, we used multiphoton time-lapse imaging methods, GH-enhanced green fluorescent protein transgenic mice and sexual dimorphism of the GH axis as a model of divergent tissue demand. Using these methods to acutely (12 h) track cell dynamics, we report that ovariectomy induces a dramatic and dynamic increase in cell motility, which is associated with gross GH-cell network remodeling. These changes can be prevented by estradiol supplementation and are associated with enhanced network connectivity as evidenced by increased coordinated GH-cell activity during multicellular calcium recordings. Furthermore, cell motility appears to be sex-specific, because reciprocal alterations are not detected in males after castration. Therefore, GH-cell motility appears to play an important role in the structural and functional pituitary plasticity, which is evoked in response to changing estradiol concentrations in the female. **(*Endocrinology* 152: 4789–4799, 2011)**

The pulsatile secretion of endocrine hormones from the pituitary gland is essential for the regulation of many important body processes, such as growth and metabolism, reproduction, and stress responses. To maintain homeostasis, endocrine cell activity must dynamically adapt to changing physiological status and environmental conditions. A key aspect of this functional adaptation is the ability of pituitary cell populations to undergo marked plasticity in response to demand, generating the appropriate tissue output in the form of hormone. It is widely acknowledged that alterations in cell number (*i.e.* hypo- or hyperplasia) (1, 2) and cell size (*i.e.* hypo- or hypertrophy) (3) represent the principal mechanisms underlying pituitary plasticity. However, due to the historic lack of techniques with which to monitor and track cell kinetics *in situ* in real time, the potential contribution of cell motility to structural and functional plasticity within the mammalian pituitary gland remains to be determined.

Recently, we have shown that the pituitary gland contributes to sex differences in GH secretion through the effects of gonadal steroids directly upon GH-cell function and output (4). The arrangement of GH-cells into a three-

ISSN Print 0013-7227 ISSN Online 1945-7170
Printed in U.S.A.

doi: 10.1210/en.2011-1430 Received June 28, 2011. Accepted September 8, 2011.
First Published Online September 27, 2011

Abbreviations: EE, Ethinylestradiol; eGFP, enhanced green fluorescent protein; ER, estrogen receptor; EthD-1, ethidium homodimer-1; OVX, ovariectomized; V/S, volume/surface.

dimensional GH-cell network that wires the gland allows coordinated propagation of information between distant cell ensembles after arrival of the hypothalamic secretagogue GHRH (4–6). Gonadal steroids target this GH-cell network, altering correlated cell activity and secretory output in response to GHRH (4). Although the mechanisms underlying this functional divergence are elusive, it may be partly due to remodeling of GH-cell network connectivity by gonadal steroids, because sex differences in GH-cell topological organization are observed during sexual maturation (4, 5).

In other tissues, such as the developing and adult brain, gonadal steroids are able to induce a range of permanent morphological changes that are important for behavioral and functional differences between the sexes. For example, estradiol induces neurite extension and influences synaptic density in a number of brain regions, perinatal exposure to the same sex steroid potently increases dendritic spine number in neurons comprising the hippocampus, ventromedial, and mediobasal hypothalamus, and brain structure dynamically changes as a function of stage of the menstrual cycle (see Refs. 7–10 and reviewed in Ref. 11). Interestingly, the permissive effects of gonadal steroids on carcinoma invasiveness are, in part, due to the promotion of motility in transformed cells. Indeed, exogenous application of estradiol has been shown to potently increase motility in both estrogen receptor (ER)-positive mammary and endometrial cells (12, 13). Despite the well-defined role of gonadal steroids in driving pituitary plasticity in response to both physiological and pathological demands in adults (2, 14–18), it remains to be shown whether they can impact cell motility to induce structural remodeling and sexually differentiated function of endocrine cell populations such as GH-cells.

We therefore investigated the motility of living pituitary cells and whether sexually dimorphic GH-cell network function in adults was associated with differential effects of gonadal steroids on GH-cell motility and structural rearrangement. To facilitate this, we took advantage of a tractable GH-cell model [GH-enhanced green fluorescent protein (eGFP)] (19), allowing us to dynamically image and track single-cell movement over a 12-h period. By subjecting acute pituitary slices derived from intact and gonadectomized GH-eGFP animals to multiphoton time-lapse imaging (12 h), we here report a role for cell motility in structural and functional pituitary plasticity.

Materials and Methods

Animals

Mice expressing GH-eGFP under the control of the human GH promoter were used in all experiments as previously described (19). Unless otherwise stated, all animals were postpubertal adults between 60 and 80 d old. Three groups of animals were used: sham, gonadectomized, and gonadectomized + hormone replacement [ethinylestradiol (EE), 0.03 mg pellet; Innovative Research of America, Sarasota, FL]. For gonadectomy experiments, mice were anesthetized by an ip injection of a ketamine (Merial, Lyon, France) (1%)/xylazine (Bayer, Leverkusen, Germany) (0.1%) mixture. In all cases, experiments were performed 6 d after surgery, a period of time shown to coincide with gross structural remodeling events after gonadectomy or hormone treatment (2, 20). To control for confounding effects of gonadal steroids on other estrogen-sensitive pituitary cell populations, such as lactotrophs, slices taken from mice expressing rat PRL-promoter driven DsRed were also imaged (21, 22). All animal studies were conducted in compliance with the animal welfare guidelines of the European Community and/or the United Kingdom Home Office, as appropriate.

Live imaging and cell motility analysis

Thick pituitary slices (200 μm) were prepared from GH-eGFP animals as previously described (5). Slices were immediately transferred to a custom made incubation chamber (37 C, 95%O_2/5%CO_2), which was mounted on the microscope stage and continuously perfused with OptiMEM medium supplemented with N2 growth complement (Invitrogen, Villebon sur Yvette, France). Dynamic cell imaging was conducted using a two-photon laser-scanning system (Trimscope; LaVision Biotec, Bielefeld, Germany) in single-beam mode and a low-magnification water-immersion objective (20X, NA 0.95 Plan Fluorite; Olympus, New York, NY). A femtosecond pulsed laser (Ti:Sapphire; Coherent, Santa Clara, CA) provided wavelengths of 910 and 970 nm to excite eGFP and DsRed, respectively. Images were captured using sensitive photomultiplier tubes and emission filters of 510 and 593 nm for eGFP and DsRed, respectively. Experiments were conducted for 12 h, and one z-stack, corresponding to 20–50 images every 2 μm along the z-axis, was acquired every 5 min from the lateral zone of the gland, because previous studies have demonstrated that sexually dimorphic alterations in GH-cell network function are most evident in this portion of the pituitary (4). Cell motility was analyzed as previously described (23). The x, y, and z coordinates of individual cells over time were obtained using Imaris Bitplane software (Bitplane, Zurich, Switzerland). Motility and sphericity parameters were calculated using Imaris or MATLAB (MathWorks, Natick, MA). The reported parameters include average speed (defined as path length over time), instantaneous speed (path length between two time points averaged over three successive time points), and sphericity (1 = a perfect sphere). Track lengths were statically encoded using Imaris on a scale from 0 to 110 μm to visually represent the path length of cells over a period of 4 h of imaging, corresponding to a 4- to 8-h timeframe after euthanasia for standardization purposes. The x, y, and z displacements of cells over a 4-h imaging period were plotted on three-dimensional plots using Chaser script for MATLAB (23).

Clustering density analysis

Individual pituitary glands from intact, ovariectomized (OVX) and OVX + EE females were imaged using a Zeiss LSM 7MP multiphoton microscope (Zeiss, Oberkochen, Germany). Volume/surface (V/S) ratios, an indicator of degree of GH-cell

clustering, were calculated as previously described using a voxel of 1024 × 1024 × 200 μm and the Imaris surface-rendering tool (Bitplane) (4, 5). Using this metric, a high ratio value corresponds to a high level of cell clustering.

Calcium imaging

To investigate whether changes in GH-cell motility were accompanied by alterations in network activity over the time course tested, calcium (Ca^{2+}) imaging was performed as previously described (4, 6). Briefly, 150-μm-thick pituitary slices were incubated for 1 h in a 20 μM solution of fura 2-AM diluted with a mixture of dimethylsulfoxide (0.01% wt/vol), 20% pluronic acid (0.005% wt/vol) (all from Invitrogen), and Ringer solution (125 mM NaCl, 2.5 mM KCl, 1.25 mM NaH_2PO_4, 26 mM $NaHCO_3$, 12 mM glucose, 2 mM $CaCl_2$, and 1 mM $MgCl_2$). For all experiments, a 300 × 300 μm area (2 × 2 binning) of the pituitary gland was imaged using a two-photon system (Trimscope; LaVision Biotec) in 64-beam fast-scan mode. Wavelengths of 780 and 910 nm were used to excite fura 2 and eGFP, respectively. Images were captured with a 14-bit back-illuminated EM-CCD camera (Andor, Belfast, Ireland) and emitted signals recorded from 468 to 552 nm for both fluorophores. Lambda scans were performed to ensure there was no overlap of the emitted fluorescence signals. Experiments were conducted for at least 30–60 min. During this time, slices were incubated at 36 C and continuously irrigated with Ringers solution aerated with 95%O_2/5%CO_2. GHRH 10 nM (Bachem, Munich, Germany) was introduced through the perfusion system for the indicated periods. After recording, GH-eGFP cells containing fura 2 were delineated with a region of interest and fluorescence over time measurements obtained using ImageJ (National Institutes of Health, Bethesda, MD). Since deflections in fura 2 emission intensity correspond to rises in cytosolic Ca^{2+} when imaged above the isosbestic point, fluorescence emission signals were inverted before normalization of Ca^{2+} traces (F/F_{min}). GHRH-responsive cells were defined as those displaying a rapid and sustained increase in intracellular Ca^{2+} concentrations of at least 20% above stable baseline levels. Ca^{2+} traces were manipulated and analyzed using custom algorithms programmed for Igor Pro (Lake Oswego, OR) and MATLAB (freely available at http://ipam.igf.cnrs.fr/).

Cell viability assay

To test cell viability in pituitary slices after 12 h of imaging, ethidium homodimer-1 (EthD-1) staining was used (Sigma-Aldrich, Saint-Quentin Fallavier, France). Cells with compromised membranes exhibit red-fluorescence from the live-cell-impermeant nucleic acid stain EthD-1 (excitation 528 nm/emission 617 nm). Slices were incubated for 20 min at 37 C in Ringers solution supplemented with 2 μM EthD-1. Treatment for 30 min with 1% Triton X-100 (Sigma-Aldrich) was used to induce cell death and determine maximum EthD-1 staining (as positive controls). Slices were subsequently fixed in 4% paraformaldehyde and imaged using a Zeiss LSM510 meta-confocal in single-track mode.

Fluorescence-activated cell sorting analysis

Fresh pituitary glands were dissected immediately after euthanasia, the neurointermediate lobe discarded, and anterior pituitary cells dispersed as previously described (3). Briefly, the pituitary glands were preincubated for 10 min in 0.05% trypsin before trituration and dispersion for 25 min in Hank's Balanced Salt Solution (pH 7.4) containing 50 caseinolytic U/ml dispase (BD Bioscience, Marseilles, France), 2.25 mg/ml collagenase A, and 25 μg/ml deoxyribonuclease (all from Sigma-Aldrich). Cells were resuspended in 0.1 M PBS and flow cytometry performed using a Coulter Epics XL-MCL flow cytometer (Beckman Coulter, Inc., Brea, CA). Data were analyzed with FlowJo software (Tree Star, Ashland, OR).

Serum LH measurement

To confirm the gonadectomized status, uterine weights and plasma LH concentrations were measured. Plasma LH values were determined by specific RIA using reagents provided by the National Institute of Diabetes and Digestive and Kidney Diseases. Samples were assayed in triplicate and the limit of detection for LH was 0.2 ng/ml of plasma.

Statistical analysis

In all experiments, data normality was tested using the D'Agostino and Pearson omnibus test. All displayed values represent the mean ± SEM from at least three independent experiments. Pairwise comparisons were made using the Mann-Whitney *U* test. Multiple comparisons were made using one-way ANOVA followed by Bonferroni's *post hoc* test. *P* values were considered significant at $P < 0.05$, $P < 0.01$, and $P < 0.001$.

Results

Gonadectomy increases GH-cell motility in females

We performed overnight three-dimensional time-lapse recordings of pituitary slices taken from postpubertal 60- to 80-d-old male or female GH-eGFP mice. Different groups of animals for each sex were used: sham, gonadectomized (OVX or castration), and gonadectomized + hormone replacement (OVX + EE in females). Uterine weight and serum LH concentrations were measured as confirmation of the effectiveness of OVX and subsequent complementation with EE. As expected, a significant decrease in uterus weight could be observed in OVX females (19 ± 2 mg *vs.* 121 ± 21 mg; OVX *vs.* sham, respectively; $P < 0.05$), which was reversed after EE complementation (97 ± 29 mg, OVX + EE, $P < 0.05$ *vs.* OVX). LH plasma levels were measured in the same conditions and, as expected, were significantly increased in the OVX animals (39.0 ± 5.0 ng/ml *vs.* 1.7 ± 0.3 ng/ml, OVX *vs.* sham, respectively, $P < 0.001$) and suppressed in the OVX + EE group (0.6 ± 0.1 ng/ml; $P < 0.001$ *vs.* OVX).

Recordings of glands removed from intact male and female animals revealed the presence of a quiescent GH-cell network, which displayed minimal structural turnover as indicated by a homogeneous distribution of cell motilities (Fig. 1 and Supplemental Videos 1 and 2, published on The Endocrine Society's Journals Online web site at http://endo.endojournals.org). Strikingly, 6 d after OVX, there

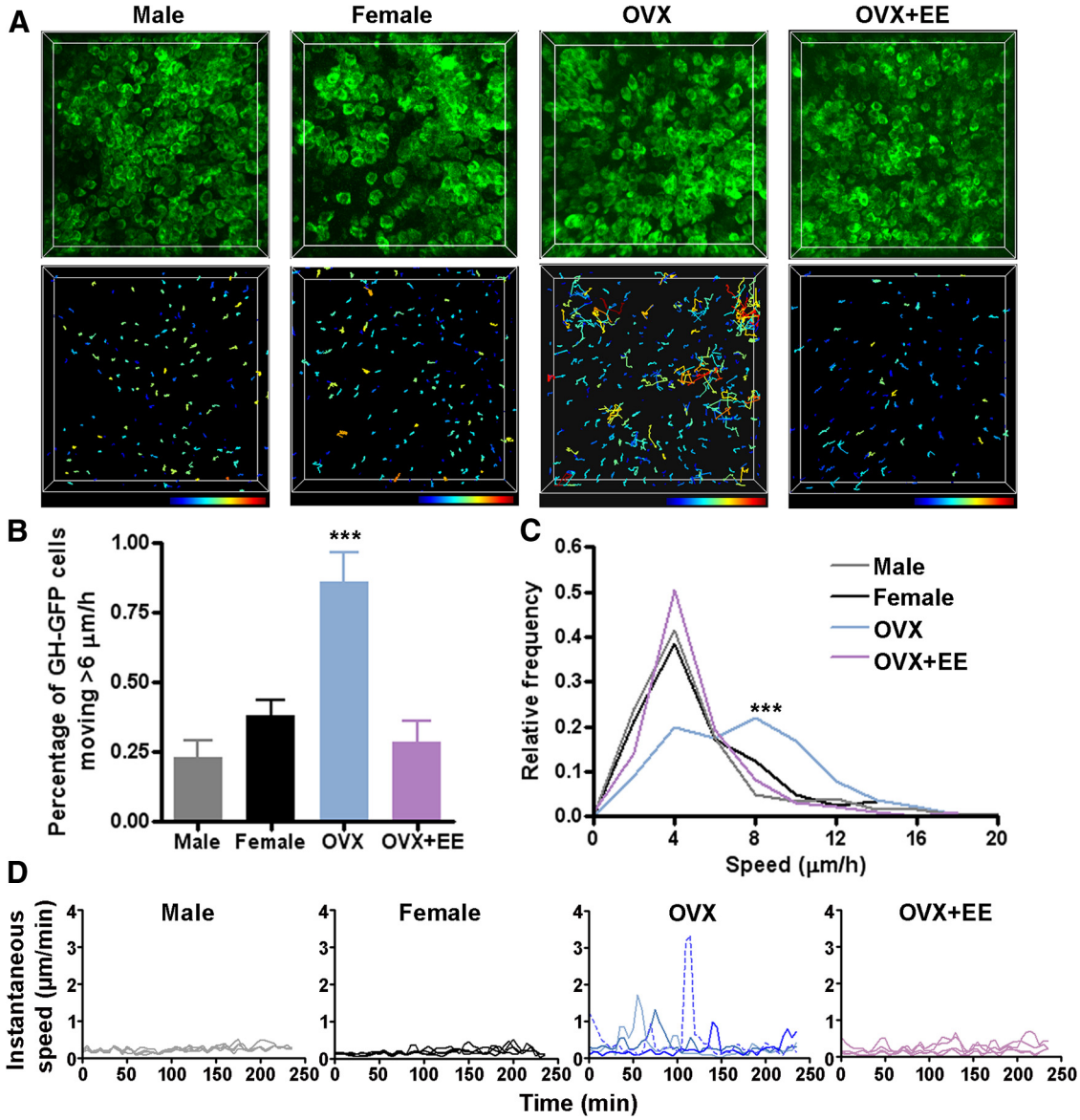

FIG. 1. OVX induces an increase in GH-cell motility. A, Representative images of the GH-cell network in the lateral lobes of pituitary slices from transgenic GH-eGFP male, female, OVX female, and OVX + EE complemented (OVX + EE) female animals acquired using a two-photon laser-scanning system (Trimscope) in single-beam mode and a femto-pulsed laser tuned to 910 nm (*top panels*). Images correspond to the projection of a 45-μm z-stack (image dimensions, 250 × 250 × 45 μm). The tracks followed by representative cells over a period of 4 h are represented for each condition (*bottom panels*). Track lengths were statically color coded using Imaris (*scale* from 0 to 110 μm). B, The average speed of the 20 most motile cells (n = 5 independent animals for each condition) was calculated using Imaris. There was a significant increase in the percentage of GH-cells moving over 6 μm/h after OVX (one-way ANOVA; ***, $P < 0.001$). Data represent mean ± SEM. The total number of GH-cells within a field was estimated by measuring the total GH-cell network volume in each z-stack image and the average volume of an individual GH-cell using the surface rendering tool in Imaris. C, The relative frequency distribution of the average speed of the cells analyzed in B was significantly different after OVX compared with the other conditions (n = 5 animals, 20 cells/animal, one-way ANOVA; ***, $P < 0.001$) and not homogenous. D, Instantaneous speed of representative cells presenting the highest motility in each condition over the course of 4-h imaging time period (n = 4 cells), showing the increase in average speed after OVX is actually due to peaks of instantaneous speed.

was a marked increase in GH-eGFP cell motility (Fig. 1 and Supplemental Video 3), which was not seen in OVX females implanted with EE pellets (Supplemental Video 4). When GH-eGFP cell motility of OVX females was directly compared with that observed in intact animals, cells were, on average, able to move over larger distances for a given time period (Fig. 1A). This translated to a larger percentage of GH-eGFP cells displaying an average speed of more than 6 μm/h in OVX females *vs.* other states (~0.8–1% compared with 0.2–0.4%) (Fig. 1B). As shown by the frequency distribution of the average speed of the most motile cells (Fig. 1C), only a subset of GH-cells displayed increased motility over the imaging period. In the other conditions, cell speeds were low and clustered around the

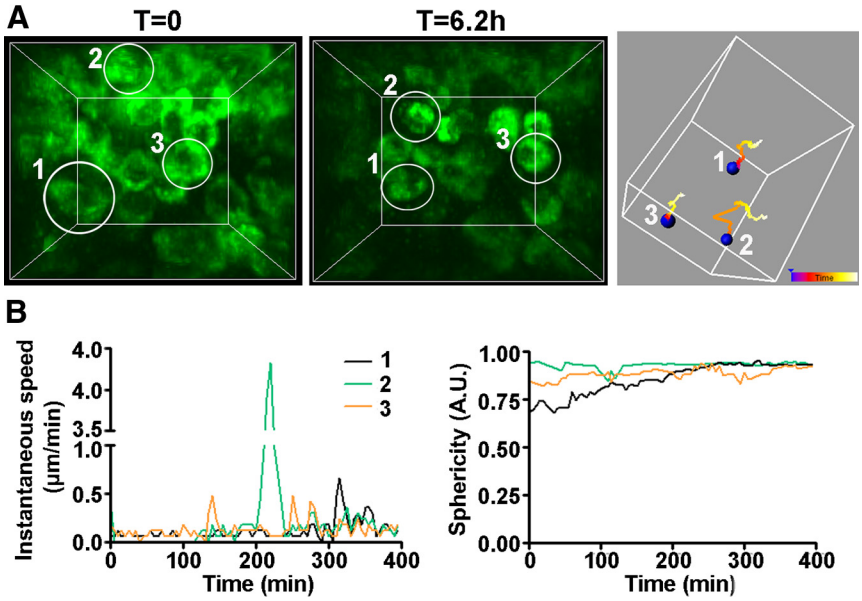

FIG. 2. Bursts in GH-cell speed are not associated with major changes in cell shape. A, High-magnification images of the GH-cell network in the lateral lobes of pituitary slices from a transgenic GH-eGFP female 6 d OVX, acquired using a two-photon microscope as described in Fig. 1. The two images were acquired at times 0 and 6.2 h, respectively, after initiation of the imaging period (*left panels*). The positions of three representative cells (cells numbered 1–3) in images corresponding to projections along the z-axis are represented (*left panels*) (image dimensions, 42 × 42 × 93 μm). *Green*, GFP. The tracks followed by the same representative cells over the imaging period are represented (*right panel*). Tracks were color coded as a function of time using Imaris. Total track lengths were 68.9, 125.1, and 83.2 μm for cells 1, 2, and 3, respectively. B, Instantaneous speed (*left panel*) and sphericity (*right panel*) of the three cells selected in A.

same value, indicating that most cell movement was slow and relatively homogeneous (Fig. 1C). Independent analysis of the instantaneous speeds of only cells displaying increased motility after OVX (*i.e.* those with an average speed of >6 μm/h) revealed that cell displacement was not constant over time but showed spikes in instantaneous speed of up to 5 μm/min. This suggests that cellular reorganization does not occur in OVX females by means of an increase in average cell speed but rather occurs as large individual steps between the start and end position (Fig. 1D). Large individual cell displacements after OVX were not synchronized or accompanied by alterations to cell shape, because the peaks of instantaneous speed were not simultaneous between the different cells (Fig. 1D), and no changes in sphericity could be detected (Fig. 2). Furthermore, cluster formation and dissociation could both be observed in the time-lapse movies after OVX (Supplemental Videos 5 and 6, respectively). Suggesting that GH-cells were not simply migrating out of the slice was the observation that cell movement did not possess a specific directionality (Fig. 3).

Changes in cell motility are not due to cell death/hyperplasia

The changes in cell motility observed after OVX did not reflect increased susceptibility of cells to phototoxicity, as there was very little uptake of EthD into nuclei after 12 h of imaging, demonstrating good cell viability (Fig. 4A). Moreover, increased motility was not due to OVX-induced cell hypo/hyperplasia, because there was no significant difference in the GH-cell content of pituitaries from sham and OVX animals 6 d after surgery (Fig. 4B).

Reciprocal alterations in cell motility are not observed after castration in males

Since testosterone has marked effects upon GH-network function and output, we investigated whether castration in males would lead to similar (or opposite) effects to those observed after OVX in females. In intact animals, there was no significant difference in basal GH-cell motility between males and females (average speed ± SEM of 5.57 ± 0.2 *vs.* 5.47 ± 0.35 μm/h, males *vs.* females, respectively; $P = 0.467$) (Fig. 1, A and B). More surprising was the observation that the effects of gonadal steroids upon cell motility appeared to be specific to females, because in males, cell movement remained unchanged 6 d after castration (average speed, 5.47 ± 0.35 *vs.* 6.25 ± 0.25 μm/h, male *vs.* castrated, respectively; $P = 0.0571$) (Fig. 5, A and B).

OVX influences GH-cell network architecture

To assess the contribution of OVX-induced cell motility to GH-cell network remodeling, we performed high resolution imaging of GH-eGFP glands removed from intact, OVX, and OVX + EE females. GH-cell network V/S ratios were significantly higher in OVX *vs.* intact females, suggesting that OVX was associated with a higher level of GH-cell clustering (Fig. 6). Similarly to the changes in cell-motility, this remodeling could be prevented by supplementing OVX animals with EE (Fig. 6).

Increased somatroph motility coincides with modification of the GH-cell network response to GHRH in females

By recording Ca^{2+}-signals emanating from the GH-eGFP cell population *in situ*, we were able to show that the structural remodeling observed in response to OVX in females was associated with heightened network function (Fig. 7, A and B). Previous studies have shown that in intact females, approximately 30% of GH-cells respond

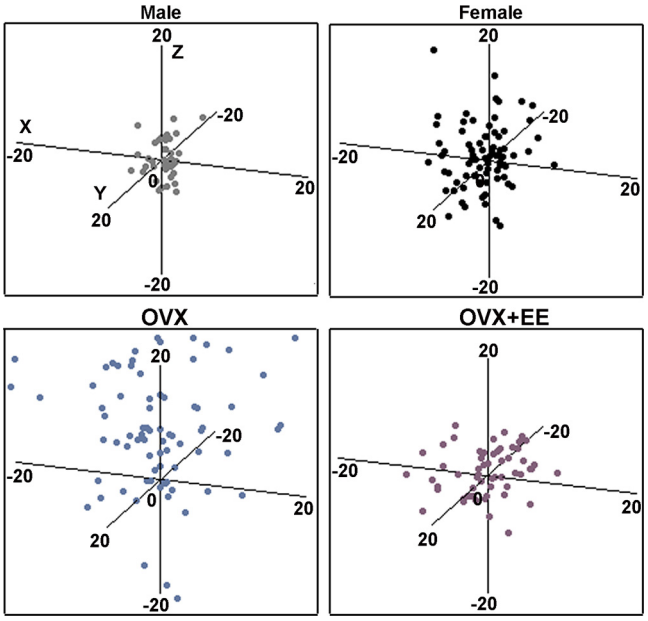

FIG. 3. Displacement of GH-cells does not present preferential directionality. The x, y, and z coordinates of the 20 most motile cells (n = 5 independent animals for each condition) were obtained using Imaris. The x, y, and z displacement of cells over the 4-h imaging period was plotted on three-dimensional plots using an open source algorithm for MATLAB. The coordinate on each axis was set to 0 for each cell at t = 0 of imaging period. *Scales* correspond to the −20 to 20 μm interval on each axis.

coordinately to secretagogue, and this percentage increases to 80% by d 15 after OVX (4). Consistent with this was the observation that, 6 d after OVX in the current study, almost 50% of GH-cells responded to GHRH by firing coordinated Ca^{2+} spikes (Fig. 7C).

Gonadal steroids do not affect lactotroph motility

We wondered whether OVX-induced motility was an inherent property only of somatrophs or could be demonstrated in other pituitary cell types (5). We chose to study lactotrophs, since we had a similar fluorescent tag in these cells. In addition, lactotrophs are known to be a highly gonadal steroid-sensitive endocrine cell population, in which proliferation, apoptosis, and function are dramatically altered by estradiol levels (3, 24–27), and they represent an abundant population in the female pituitary (28). Furthermore, PRL- and GH-cell networks are tightly intermingled, so the reorganization of one cell network might also influence the other. However, in imaging studies using pituitary slices from PRL-DsRed transgenic mice, we observed no alterations in the motility of lactotrophs after OVX. PRL-DsRed cells displayed little displacement over long periods of imaging (Fig. 8A), and the average speed of even the most motile PRL-DsRed cells from five independent experiments in PRL-DsRed OVX females was not significantly different from that of GH-eGFP cells in intact animals (Fig. 8B). Therefore, changes in somatroph motility after OVX do not simply reflect an increase in general motility of estradiol-sensitive pituitary cells after gonadal steroid removal.

Discussion

To allow functional adaptation to changing environmental conditions, the pituitary gland has evolved to be a highly plastic organ in mammals. Currently, the principal mechanisms considered to underlie endocrine cell plasticity in the pituitary are alterations in cell number and size. However, in other organs, changes in cell movement represent a third mechanism, which contributes to tissue plasticity (29). The pituitary gland has traditionally been regarded as a rather static organ, but using multiphoton time-lapse imaging methods, we clearly show the existence of cell motility in the GH-cell population and that it is altered during bouts of structural and functional pituitary plasticity in females in response to changes in the ovarian steroid milieu.

Previous studies by our group have shown that after OVX in adult females, GH-cell network responses to secretagogue administration are amplified and can be reversed with estradiol (EE) replacement. By tracking cell kinetics in real time, we were unable to see significant major changes in GH-cell network structure over timescales of a few hours in intact animals. By contrast, 6 d after OVX in females, there was a large and rapid (minutes to hours) enhancement of GH-cell motility, which was associated with GH-cell network remodel-

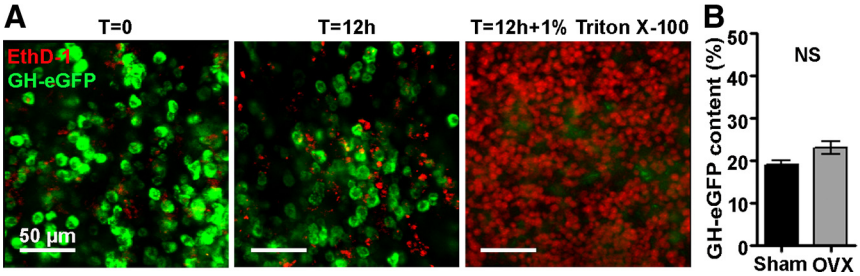

FIG. 4. GH-cell network remodeling is not due to cell death or hyperplasia. A, Representative confocal images of fixed, EthD-1 (*red*) stained slices from OVX GH-eGFP (*green*) females immediately after euthanasia (*left panel*), after 12 h of imaging (*middle panel*), or after a 30-min treatment with 1% Triton X-100 to induce cell death (*right panel*). No differential staining could be observed before and after imaging nor between the different experimental conditions (male, female, OVX, and OVX + EE). Image dimensions, 230 × 230 × 10 μm. B, Flow cytometry analysis of the GH-cell content of whole pituitary glands from GH-eGFP female and OVX female animals (n = 4). At least 100,000 dispersed cells were analyzed. No significant difference (NS) could be observed (Mann-Whitney test, $P > 0.05$). Data represent mean ± SEM.

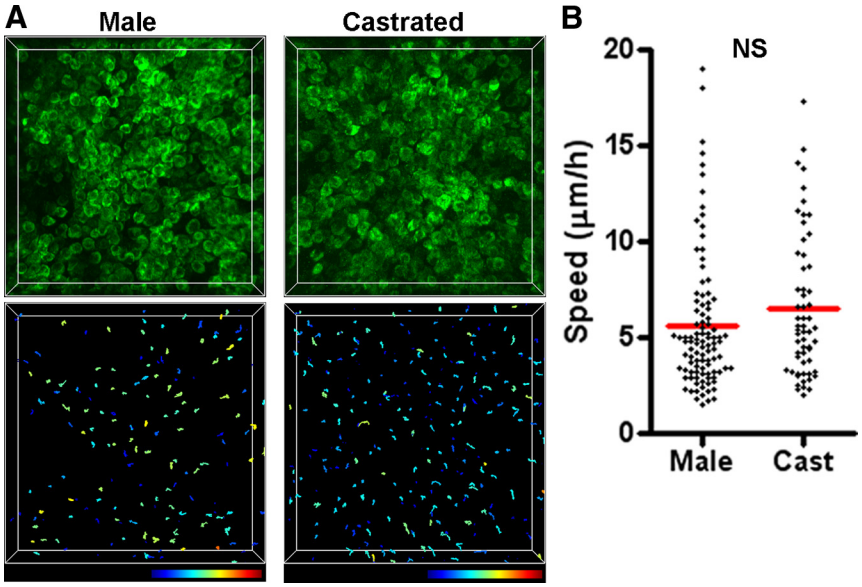

FIG. 5. Gonadectomy in males does not induce changes in GH-cell motility. A, Representative images of the GH-cell network in the lateral lobes of pituitary slices from transgenic GH-eGFP male and castrated (Cast) male animals acquired using a two-photon microscope as described in Fig. 1 (*top panels*). Images correspond to the projection of a 45-μm z-stack (image dimensions, 250 × 250 × 45 μm). The tracks followed by representative cells over a period of 4 h are represented for each condition (*bottom panels*). Track lengths were statically color coded using Imaris (*scale* from 0 to 110 μm). B, The average speed of the 20 most motile cells (n = 3–5 independent animals for each condition) were calculated using Imaris. No significant difference (NS) could be observed (Mann-Whitney test, $P > 0.05$). Data represent mean ± SEM.

ing as evidenced by increased GH-cell clustering. These OVX-induced changes in GH-cell motility and network remodeling could be prevented with prior EE supplementation and coincided with moderately enhanced GH-cell network function in the form of coordinated Ca^{2+}-spiking activity. As such, these data suggest that a reduction in E2 resulting from OVX may promote rapid structural remodeling and enhanced cell-cell connectivity through a transient increase in cell motility, consistent with its effects on GH-cell network connectivity and function (4). It should be noted that no differences in basal GH-cell motility were detected between the sexes. Therefore, our findings reflect a dynamic response to hormonal status and cannot be related to normal patterns of GH secretion but rather changes in network structure that then impact secretion. Nevertheless, these data are consistent with *in vivo* studies in rodents showing that OVX leads to larger male-like nocturnal GH pulses (30). Presumably, sex differences in GH-cell network function (4, 5) are programmed through either transient or prolonged increases in cell motility occurring around the time of sexual maturation and do not require further changes in cell motility for maintenance of structural connectivity in adults.

The effects of estrogens on cell motility are well characterized in other systems, with potent effects on tumorigenesis and metastasis. High doses of estradiol have been shown to influence expression patterns of adhesion molecules and may alter cell-matrix interactions, resulting in loss of cell adhesion (31). An increase in actin remodeling may also lead to formation of membrane structures, which favor cell migration (32). The mechanisms underlying the increased GH-cell motility after OVX and estradiol withdrawal remain unknown. However, previous studies have shown that estradiol inhibits the invasive potential of some ovarian cancer cell lines (33, 34) and prevents prostaglandin E2-induced cellular motility of human colon cancer cells (35). Since there are specific cadherin expression patterns in pituitary GH-cells (36), it is reasonable to speculate that estradiol withdrawal may directly or indirectly alter these to promote an increase in GH-cell motility.

The increase we observed in cell motility after OVX was relatively specific for GH-cells and thus unlikely to be due to a generalized nonspecific effect of estradiol such as induction of cell death/fragility or hyperplasia (because the GH-cell content was comparable in intact and OVX females). Although OVX may have conceivably resulted in an increase in GH-cell proliferation rate, which was balanced by an increase in cell death, leading to enhanced cell motility and structural remodeling, available evidence suggests otherwise: estradiol tends to sensitize pituitary cells to proapoptotic and mitogenic signals (27, 37), the GH-cell population is remarkably stable (*i.e.* there is no trans-differentiation into mammo-GH-cells) during periods of high estradiol concentrations in mice (3), and only approximately 3% of GH-cells in female rodents are immunoreactive for ERα, the membrane receptor subtype predominantly expressed in the anterior pituitary and which is implicated in rapid apoptotic effects of estradiol (38–40). It cannot be excluded that a change in GH-cell kinetics observed after OVX might be secondary to similar changes in other networks. We believe we can rule out the PRL-network, as the neighboring lactotrophs remained static under the same conditions. Another obvious population, although much smaller in number, would be pituitary gonadotrophs, whose activity and potential mobility might well be expected to increase in response to the gonadectomy-induced GnRH surge (41). If so, it might also be expected to alter somatotroph motility in males, but such changes were not observed. Nevertheless, animals with tagged LH/FSH-secreting cells have recently become available (42,

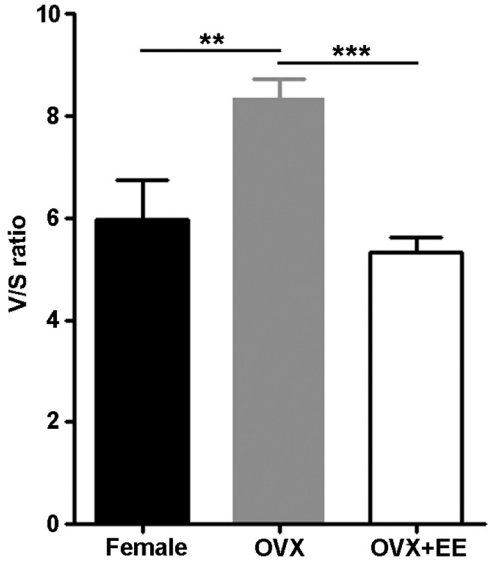

FIG. 6. OVX induces GH-cell network remodeling in females. Effect of OVX and OVX + hormone replacement on the V/S ratio of the GH-cell network in female GH-eGFP mice. A significant increase in the V/S ratio was observed after OVX. These changes in V/S are prevented if animals are supplemented with EE at the time of OVX (6–10 surface rendering of high-resolution images of the GH-cell network of dimension 1024 × 1024 × 200 μm were used for each group, one-way ANOVA; **, $P < 0.01$ and ***, $P < 0.001$). Data represent mean ± SEM).

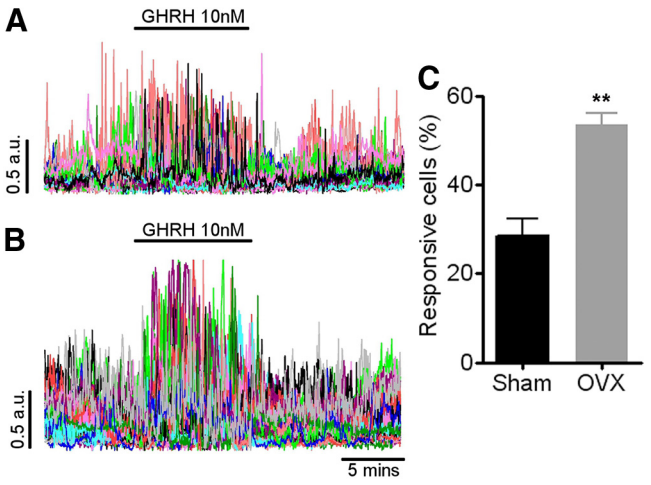

FIG. 7. Increased GH-cell motility coincides with modification of GH-cell network response in females. A, Calcium (Ca^{2+}) imaging was performed using a two-photon microscope in multiplexed (64 beam) mode and a laser tuned to 780 nm (field 300 × 300 μm, ~100 imaged cells; 2 × 2 binning). Acute pituitary slice preparations from intact GH-eGFP females were prepared and loaded with the Ca^{2+}-sensor, fura 2. GHRH (10 nM) was perfused onto the slice for the indicated time period. GH-eGFP cells coloaded with fura 2 were postidentified in ImageJ with a region of interest and intensity over time measurements plotted (a.u. = arbitary intensity units). Note that in intact animals, cells responded to GHRH input by firing highly coordinated Ca^{2+} spikes. B, As for A but from pituitary slices obtained from OVX females. A greater proportion of cells responded to application of the same dose of GHRH. C, The number of cells that coordinately respond to GHRH application was significantly higher 6 d after OVX (n = 7 slices from four animals for each condition, Mann-Whitney test; **, $P < 0.01$). Data represent mean ± SEM.

43), so it could be interesting to directly study gonadotroph motility. Other possible indirect effects could include vascular or folliculostellate cell remodeling (44), but again, there is no evidence suggesting that this would be relatively cell and/or sex specific. We prefer the simpler hypothesis that motility in the GH-cell network contributes to the gonadal-sensitive structural and functional plasticity that we have previously demonstrated in female mice (4).

Only a subpopulation of GH-cells could be shown to be involved in network remodeling events over our imaging period, indicating that cells comprising the GH-cell network are differentially responsive to OVX. There are a number of nonmutually exclusive explanations for this observation. First, OVX may only be able to activate intracellular pathways involved in cell migration in a subset of cells due to the aforementioned low levels of ER expression by somatrophs. Second, studies using estradiol-deficient aromatase knockout mice implicate estrogens in the normal expression of GHRH receptors, which would confer GH-cell specificity (45). Underexpression of GHRH receptors restricted to a subpopulation of ER-expressing GH-cells could lead to loss of situational awareness. Indeed, GHRH signaling is essential for cell proper placement within the GH-cell network during development, because animals deficient in GHRH suffer severe GH-cell hypoplasia and a loss of cell clustering (46). Equally plausible is a GH-cell-specific role for estrogens in regulating the balance between GHRH and somatostatin receptors. Somatostatin has long been known to restrain GH-cell activity (47), so it is possible that somatostatin receptors may also be involved in restraining cell motility, and reducing their expression by removing endogenous estrogens would lessen this effect (48). Third, OVX may result in regional changes in chemo-attractant concentrations through changes in the paracrine output of neighboring estrogen-sensitive cell types, such as lactotrophs (49, 50). Fourth, remodeling may progressively occur over several days, so we may not capture the full extent of GH-cell motility using the current methods. Together, these mechanisms would account for the restriction of cell motility to only 1% of the imaged GH-cell network and provide a potential explanation for movement of both ER- and non-ER-expressing GH-cells.

The large change in GH-cell network function (20%) may not only be associated with an increase in motility of a small proportion (1%) of GH-cells. Since animals were OVX on d 1 and experiments conducted for a 12-h window on d 6, a higher proportion of cells may have moved before the recording period but subsequently become immotile. This is supported by the fact that large individual

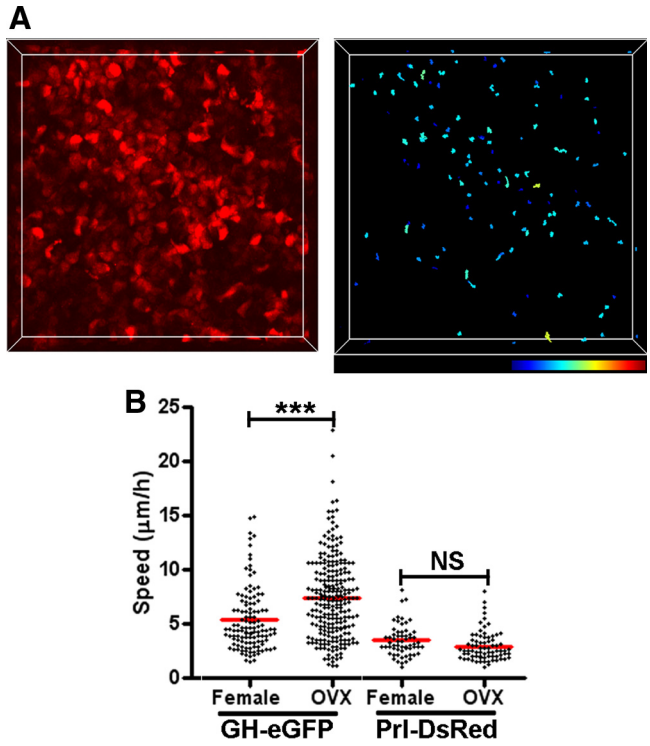

FIG. 8. Gonadectomy does not induce lactotroph motility. A, Representative image of lactotrophs occupying the lateral lobes of pituitary slices taken from intact and OVX PRL-DsRed mice and acquired using a two-photon microscope as described in Fig. 1 but with a laser tuned to 970 nm (*left panel*). Image corresponds to the projection of a 45-μm z-stack (image dimensions, 250 × 250 × 45 μm). The tracks followed by representative cells over a period of 4 h are represented for an OVX female (*right panel*). Track lengths were statistically color coded using Imaris (*scale* from 0 to 110 μm). B, The average speed of the 20 most motile cells (n = 5 independent animals for each condition) was calculated using Imaris. No significant difference in PRL-DsRed cell motility could be observed between the sham and OVX females (Mann-Whitney test, $P > 0.05$). Data were compared with those from control and OVX GH-eGFP cells and represented as mean ± SEM.

cell displacements after OVX were rarely synchronized and that high-resolution imaging of GH-eGFP glands demonstrated a dramatic effect of OVX on GH-cell network remodeling in terms of GH-cell clustering, which can be blocked by EE. We have previously shown that GH-cell clustering is an important indicator of connectivity as determined by measurement of coordinated cell activity (4, 5). It is also possible that because correlated activity in the GH-cell network is dictated by a small number of GH-cells (4–6), a change in motility of a small proportion of cells could conceivably result in the connectivity required to produce such correlation patterns.

Although acute pituitary slice preparations were imaged *ex vivo*, outside of the influence of hypothalamic stimulation, we cannot fully exclude that the increased cell motility observed in OVX females was due to effects of estrogens at the level of GHRH neurons. Indeed, changes in cell motility could have been preprogrammed through chronic changes in estrogen-responsive GHRH input to the pituitary gland over the 6-d period after OVX. Further experiments involving *in vivo* ablation of GHRH neurons in adult OVX + EE animals would be required to further delineate this, as simply applying exogenous estradiol to slices taken from OVX animals would not reflect the chronic nature of the treatment paradigms used.

Supporting a role for estradiol and not testosterone in GH-cell motility was the observation that the GH-cell population remained static over the recording period in gonadectomized males. Therefore, previous reports showing that castration attenuates GH-cell network function (4) may reflect activational effects of testosterone on GH-cell secretory activity. The mechanisms by which testosterone promotes GH-cell function and output in males are not well defined, although it could involve permissive effects of androgens on GH-cell proliferation, GH-cell secretory capacity, and pituitary ghrelin content, a potent GH secretagogue (51–54).

Similar live-imaging studies of both dispersed cells and acute slice preparations have demonstrated that pituitary gonadotrophs extend processes and spatially reposition themselves toward blood vessels in response to exogenous GnRH application (41). Furthermore, static confocal studies have provided evidence that both gonadotrophs and corticotrophs contact vessels during periods of peak secretory demand (55, 56). Therefore, cell motility appears to be an intrinsic property of cell populations comprising the mammalian pituitary gland. In the present study, we were unable to detect obvious changes in cell morphology, such as formation of pseudopods/extension of processes. However, this may be a consequence of the spatial (axial resolution of 1.41 μm; z-step = 2 μm) and temporal resolutions (one acquisition every 5 min), which may be insufficient to detect cytoskeletal changes. Further studies using higher magnification/higher numerical aperture objectives and faster acquisition rates would be required to clarify this issue.

In conclusion, by using time-lapse microscopy to image acute pituitary slices prepared from GH-eGFP mice, we provide evidence that GH-cells move and that this motility is acutely and transiently enhanced by OVX in mice. This could directly contribute to the ability of estrogens to remodel the GH-cell network both structurally and functionally. Our data provide new insights into the mechanisms underlying estrogen-induced plasticity at the level of the pituitary gland.

Acknowledgments

We thank the animal facility staff at the Institute of Functional Genomics and, in particular, Ségolène Debiesse, Jennifer Guil-

lemin, and Dominique Haddou for technical assistance. We also thank Pierre Fontanaud for invaluable assistance with data analysis. RIA reagents were generously supplied by Dr. A. F. Parlow and The National Institute of Diabetes and Digestive and Kidney Diseases' National Hormone and Peptide Program (University of California, Los Angeles, CA).

Address all correspondence and requests for reprints to: Dr. Patrice Mollard, Department of Endocrinology, Institute of Functional Genomics, Montpellier 34094, France. E-mail: patrice.mollard@igf.cnrs.fr.

This work was supported by Agence Nationale de la Recherche (Pit-Net), Institut National de la Santé et de la Recherche Médicale, Centre National de la Recherche Scientifique, the Universities of Montpellier 1 and 2, National Biophotonics and Imaging Platform (Ireland), Fondation pour la Recherche Medicale, Réseau National des Génopoles, Institut Fédératif de Recherches no. 3, Région Languedoc Roussillon, and the Medical Research Council (United Kingdom).

Disclosure Summary: The authors have nothing to disclose.

References

1. **Nolan LA, Thomas CK, Levy A** 2004 Permissive effects of thyroid hormones on rat anterior pituitary mitotic activity. J Endocrinol 180:35–43
2. **Nolan LA, Levy A** 2006 A population of non-luteinising hormone/non-adrenocorticotrophic hormone-positive cells in the male rat anterior pituitary responds mitotically to both gonadectomy and adrenalectomy. J Neuroendocrinol 18:655–661
3. **Castrique E, Fernandez-Fuente M, Le Tissier P, Herman A, Levy A** 2010 Use of a prolactin-Cre/ROSA-YFP transgenic mouse provides no evidence for lactotroph transdifferentiation after weaning, or increase in lactotroph/somatotroph proportion in lactation. J Endocrinol 205:49–60
4. **Sanchez-Cardenas C, Fontanaud P, He Z, Lafont C, Meunier AC, Schaeffer M, Carmignac D, Molino F, Coutry N, Bonnefont X, Gouty-Colomer LA, Gavois E, Hodson DJ, Le Tissier P, Robinson IC, Mollard P** 2010 Pituitary growth hormone network responses are sexually dimorphic and regulated by gonadal steroids in adulthood. Proc Natl Acad Sci USA 107:21878–21883
5. **Bonnefont X, Lacampagne A, Sanchez-Hormigo A, Fino E, Creff A, Mathieu MN, Smallwood S, Carmignac D, Fontanaud P, Travo P, Alonso G, Courtois-Coutry N, Pincus SM, Robinson IC, Mollard P** 2005 Revealing the large-scale network organization of growth hormone-secreting cells. Proc Natl Acad Sci USA 102:16880–16885
6. **Hodson DJ, Molino F, Fontanaud P, Bonnefont X, Mollard P** 2010 Investigating and modelling pituitary endocrine network function. J Neuroendocrinol:1217–1225
7. **Griffin GD, Flanagan-Cato LM** 2008 Estradiol and progesterone differentially regulate the dendritic arbor of neurons in the hypothalamic ventromedial nucleus of the female rat (*Rattus norvegicus*). J Comp Neurol 510:631–640
8. **Schwarz JM, Liang SL, Thompson SM, McCarthy MM** 2008 Estradiol induces hypothalamic dendritic spines by enhancing glutamate release: a mechanism for organizational sex differences. Neuron 58:584–598
9. **Pletzer B, Kronbichler M, Aichhorn M, Bergmann J, Ladurner G, Kerschbaum HH** 2010 Menstrual cycle and hormonal contraceptive use modulate human brain structure. Brain Res 1348:55–62
10. **Protopopescu X, Butler T, Pan H, Root J, Altemus M, Polanecsky M, McEwen B, Silbersweig D, Stern E** 2008 Hippocampal structural changes across the menstrual cycle. Hippocampus 18:985–988
11. **McCarthy MM** 2008 Estradiol and the developing brain. Physiol Rev 88:91–124
12. **Saji S, Kawakami M, Hayashi S, Yoshida N, Hirose M, Horiguchi S, Itoh A, Funata N, Schreiber SL, Yoshida M, Toi M** 2005 Significance of HDAC6 regulation via estrogen signaling for cell motility and prognosis in estrogen receptor-positive breast cancer. Oncogene 24:4531–4539
13. **Gentilini D, Busacca M, Di Francesco S, Vignali M, Viganò P, Di Blasio AM** 2007 PI3K/Akt and ERK1/2 signalling pathways are involved in endometrial cell migration induced by 17β-estradiol and growth factors. Mol Hum Reprod 13:317–322
14. **Hunt TE** 1946 Mitotic activity in the rat hypophysis after injection of estrogenic and luteal hormones. Anat Rec 94:519
15. **Kineman RD, Henricks DM, Faught WJ, Frawley LS** 1991 Fluctuations in the proportions of growth hormone- and prolactin-secreting cells during the bovine estrous cycle. Endocrinology 129:1221–1225
16. **Oishi Y, Okuda M, Takahashi H, Fujii T, Morii S** 1993 Cellular proliferation in the anterior pituitary gland of normal adult rats: influences of sex, estrous cycle, and circadian change. Anat Rec 235:111–120
17. **Gorski J, Wendell D, Gregg D, Chun TY** 1997 Estrogens and the genetic control of tumor growth. Prog Clin Biol Res 396:233–243
18. **Nolan LA, Levy A** 2006 The effects of testosterone and oestrogen on gonadectomised and intact male rat anterior pituitary mitotic and apoptotic activity. J Endocrinol 188:387–396
19. **Magoulas C, McGuinness L, Balthasar N, Carmignac DF, Sesay AK, Mathers KE, Christian H, Candeil L, Bonnefont X, Mollard P, Robinson IC** 2000 A secreted fluorescent reporter targeted to pituitary growth hormone cells in transgenic mice. Endocrinology 141:4681–4689
20. **Nolan LA, Levy A** 2009 Prolonged oestrogen treatment does not correlate with a sustained increase in anterior pituitary mitotic index in ovariectomized Wistar rats. J Endocrinol 200:301–309
21. **Lafont C, Desarménien MG, Cassou M, Molino F, Lecoq J, Hodson D, Lacampagne A, Mennessier G, El Yandouzi T, Carmignac D, Fontanaud P, Christian H, Coutry N, Fernandez-Fuente M, Charpak S, Le Tissier P, Robinson IC, Mollard** 2010 Cellular in vivo imaging reveals coordinated regulation of pituitary microcirculation and GH cell network function. Proc Natl Acad Sci USA 107:4465–4470
22. **He Z, Fernandez-Fuente M, Strom M, Cheung L, Robinson IC, Le Tissier P** 2011 Continuous on-line monitoring of secretion from rodent pituitary endocrine cells using fluorescent protein surrogate markers. J Neuroendocrinol 23:197–207
23. **Schaeffer M, Han SJ, Chtanova T, van Dooren GG, Herzmark P, Chen Y, Roysam B, Striepen B, Robey EA** 2009 Dynamic imaging of T cell-parasite interactions in the brains of mice chronically infected with Toxoplasma gondii. J Immunol 182:6379–6393
24. **Wynick D, Small CJ, Bacon A, Holmes FE, Norman M, Ormandy CJ, Kilic E, Kerr NC, Ghatei M, Talamantes F, Bloom SR, Pachnis V** 1998 Galanin regulates prolactin release and lactotroph proliferation. Proc Natl Acad Sci USA 95:12671–12676
25. **Heaney AP, Fernando M, Melmed S** 2002 Functional role of estrogen in pituitary tumor pathogenesis. J Clin Invest 109:277–283
26. **Pisera D, Candolfi M, Navarra S, Ferraris J, Zaldivar V, Jaita G, Castro MG, Seilicovich A** 2004 Estrogens sensitize anterior pituitary gland to apoptosis. Am J Physiol Endocrinol Metab 287:E767–E771
27. **Jaita G, Candolfi M, Zaldivar V, Zárate S, Ferrari L, Pisera D, Castro MG, Seilicovich A** 2005 Estrogens up-regulate the Fas/FasL apoptotic pathway in lactotropes. Endocrinology 146:4737–4744
28. **Leong DA, Lau SK, Sinha YN, Kaiser DL, Thorner MO** 1985 Enumeration of lactotropes and somatotropes among male and female pituitary cells in culture: evidence in favor of a mammosomatotrope subpopulation in the rat. Endocrinology 116:1371–1378

29. **Friedl P, Wolf K** 2010 Plasticity of cell migration: a multiscale tuning model. J Cell Biol 188:11–19
30. **Clark RG, Carlsson LM, Robinson IC** 1987 Growth hormone secretory profiles in conscious female rats. J Endocrinol 114:399–407
31. **DePasquale JA, Samsonoff WA, Gierthy JF** 1994 17-β-Estradiol induced alterations of cell-matrix and intercellular adhesions in a human mammary carcinoma cell line. J Cell Sci 107(Pt 5):1241–1254
32. **Simoncini T, Scorticati C, Mannella P, Fadiel A, Giretti MS, Fu XD, Baldacci C, Garibaldi S, Caruso A, Fornari L, Naftolin F, Genazzani AR** 2006 Estrogen receptor α interacts with Gα13 to drive actin remodeling and endothelial cell migration via the RhoA/Rho kinase/moesin pathway. Mol Endocrinol 20:1756–1771
33. **Rochefort H, Platet N, Hayashido Y, Derocq D, Lucas A, Cunat S, Garcia M** 1998 Estrogen receptor mediated inhibition of cancer cell invasion and motility: an overview. J Steroid Biochem Mol Biol 65:163–168
34. **Hayashido Y, Lucas A, Rougeot C, Godyna S, Argraves WS, Rochefort H** 1998 Estradiol and fibulin-1 inhibit motility of human ovarian- and breast-cancer cells induced by fibronectin. Int J Cancer 75:654–658
35. **Lai TY, Chen LM, Lin JY, Tzang BS, Lin JA, Tsai CH, Lin YM, Huang CY, Liu CJ, Hsu HH** 2010 17β-Estradiol inhibits prostaglandin E2-induced COX-2 expressions and cell migration by suppressing Akt and ERK1/2 signaling pathways in human LoVo colon cancer cells. Mol Cell Biochem 342:63–70
36. **Chauvet N, El-Yandouzi T, Mathieu MN, Schlernitzauer A, Galibert E, Lafont C, Le Tissier P, Robinson IC, Mollard P, Coutry N** 2009 Characterization of adherens junction protein expression and localization in pituitary cell networks. J Endocrinol 202:375–387
37. **Seilicovich A** 2010 Cell life and death in the anterior pituitary gland: role of oestrogens. J Neuroendocrinol 22:758–764
38. **Shupnik MA** 2002 Oestrogen receptors, receptor variants and oestrogen actions in the hypothalamic-pituitary axis. J Neuroendocrinol 14:85–94
39. **Zárate S, Jaita G, Zaldivar V, Radl DB, Eijo G, Ferraris J, Pisera D, Seilicovich A** 2009 Estrogens exert a rapid apoptotic action in anterior pituitary cells. Am J Physiol Endocrinol Metab 296:E664–E671
40. **Zárate S, Seilicovich A** 2010 Estrogen receptors and signaling pathways in lactotropes and somatotropes. Neuroendocrinology 92:215–223
41. **Navratil AM, Knoll JG, Whitesell JD, Tobet SA, Clay CM** 2007 Neuroendocrine plasticity in the anterior pituitary: gonadotropin-releasing hormone-mediated movement *in vitro* and *in vivo*. Endocrinology 148:1736–1744
42. **Wen S, Schwarz JR, Niculescu D, Dinu C, Bauer CK, Hirdes W, Boehm U** 2008 Functional characterization of genetically labeled gonadotropes. Endocrinology 149:2701–2711
43. **Budry L, Lafont C, El Yandouzi T, Chauvet N, Conéjero G, Drouin J, Mollard P** 2011 Related pituitary cell lineages develop into interdigitated 3D cell networks. Proc Natl Acad Sci USA 108:12515–12520
44. **Fauquier T, Guérineau NC, McKinney RA, Bauer K, Mollard P** 2001 Folliculostellate cell network: a route for long-distance communication in the anterior pituitary. Proc Natl Acad Sci USA 98:8891–8896
45. **Yan M, Jones ME, Hernandez M, Liu D, Simpson ER, Chen C** 2004 Functional modification of pituitary somatotropes in the aromatase knockout mouse and the effect of estrogen replacement. Endocrinology 145:604–612
46. **Waite E, Lafont C, Carmignac D, Chauvet N, Coutry N, Christian H, Robinson I, Mollard P, Le Tissier P** 2010 Different degrees of somatotroph ablation compromise pituitary growth hormone cell network structure and other pituitary endocrine cell types. Endocrinology 151:234–243
47. **Holl RW, Thorner MO, Leong DA** 1988 Intracellular calcium concentration and growth hormone secretion in individual somatotropes: effects of growth hormone-releasing factor and somatostatin. Endocrinology 122:2927–2932
48. **Xu Y, Song J, Berelowitz M, Bruno JF** 1996 Estrogen regulates somatostatin receptor subtype 2 messenger ribonucleic acid expression in human breast cancer cells. Endocrinology 137:5634–5640
49. **Maus MV, Reilly SC, Clevenger CV** 1999 Prolactin as a chemoattractant for human breast carcinoma. Endocrinology 140:5447–5450
50. **Denef C** 2008 Paracrinicity: the story of 30 years of cellular pituitary crosstalk. J Neuroendocrinol 20:1–70
51. **Ho KY, Thorner MO, Krieg Jr RJ, Lau SK, Sinha YN, Johnson ML, Leong DA, Evans WS** 1988 Effects of gonadal steroids on somatotroph function in the rat: analysis by the reverse hemolytic plaque assay. Endocrinology 123:1405–1411
52. **Pagotto U, Gambineri A, Pelusi C, Genghini S, Cacciari M, Otto B, Castañeda T, Tschöp M, Pasquali R** 2003 Testosterone replacement therapy restores normal ghrelin in hypogonadal men. J Clin Endocrinol Metab 88:4139–4143
53. **Kamegai J, Tamura H, Shimizu T, Ishii S, Tatsuguchi A, Sugihara H, Oikawa S, Kineman RD** 2004 The role of pituitary ghrelin in growth hormone (GH) secretion: GH-releasing hormone-dependent regulation of pituitary ghrelin gene expression and peptide content. Endocrinology 145:3731–3738
54. **Nass R, Gaylinn BD, Thorner MO** 2011 The role of ghrelin in GH secretion and GH disorders. Mol Cell Endocrinol 340:10–14
55. **Childs GV** 1985 Shifts in gonadotropin storage in cultured gonadotropes following GnRH stimulation, in vitro. Peptides 6:103–107
56. **Itoh J, Serizawa A, Kawai K, Ishii Y, Teramoto A, Osamura RY** 2003 Vascular networks and endothelial cells in the rat experimental pituitary glands and in the human pituitary adenomas. Microsc Res Tech 60:231–235